Engine A/F and Torque Control using Secondary Throttles

Jun-Mo Kang*and Jessy W. Grizzle†
Department of Electrical Engineering and Computer Science, University of Michigan

Abstract

The proper functioning of a catalytic converter requires precise regulation of A/F to the stoichiometric value. The control of A/F is usually based on regulating the fuel flow in proportion to air flow changes imposed by the driver. However, due to the relatively long time delays in the fuel feedback loop, the controller cannot properly compensate for rapid air flow changes. To overcome this deficiency, the possibility of air flow control has been suggested by implementing secondary throttles in the intake runners. In this paper, a new structure for A/F and torque control is proposed to enhance the global performance of a secondary throttles engine.

1 Introduction and Motivation

The main dynamics for which the A/F controller should compensate are the fuel and air dynamics in the intake manifold and the transport and process delay owing to the event based nature of the engine. In particular, the air dynamics in the intake manifold is highly nonlinear, and has fast transients in normal driving conditions. To keep up with these fast transients, the A/F controller should have a high bandwidth. This is typically achieved through a combination of feedforward (fast, based on air measurement) and feedback (slow, based on feedgas oxygen level) control. However, even if the feedforward term is "perfect", the current A/F controller cannot compensate fully for these fast transients. This is because fuel injection is performed on a closed intake valve, and thus the fuel computation and scheduling must be performed at least 360^o of crankangle rotation before the air change is injested into the cylinder. To overcome this difficulty, air flow control has been studied : through an electronic throttle in [1] or [4], for example, or based on the introduction of secondary throttles in the intake runners [10].

This paper extends the work of [9], where a nonlinear engine model was linearized around specific equilibrium points, and an LQG/LTR multivariable linear controller was designed and simulated. The designed controller demonstrated satisfactory A/F excursions and transient torque response around the operating points. However, the linear controller inevitably loses control authority over the cylinder air charge at low primary throttle angles.

Figure 1 shows the steady state equilibrium points of the mass air flow rate at an engine speed of 300 rad/sec. As can be seen, at low primary throttle angles, variation of the secondary throttles hardly affects the mass air flow rate into the cylinders [9]. This is illustrated in Figure 2, where the secondary throttles drift after a tip-out, owing to the loss of control authority. Another issue is that the fast transient response of manifold pressure to a large tip-in excites the system's nonlinearities, and this has proven difficult to treat by gain scheduling.

To overcome some of the deficiencies of linear control, a combined nonlinear feedforward feedback control approach is pursued in this paper. An overview of the nonlinear engine model is presented in the next section. The controller's architecture and design are discussed in Section 3. The designed control law is evaluated via simulations in Section 4. Conclusions and future directions are disscussed in Section 5.

*Email: junmo@eecs.umich.edu

†4221 EECS Building, University of Michigan, 1301 Beal Avenue, Ann Arbor, MI 48109-2122, Tel: 313-763-3598, FAX: 313-763-8041, Email: grizzle@eecs.umich.edu

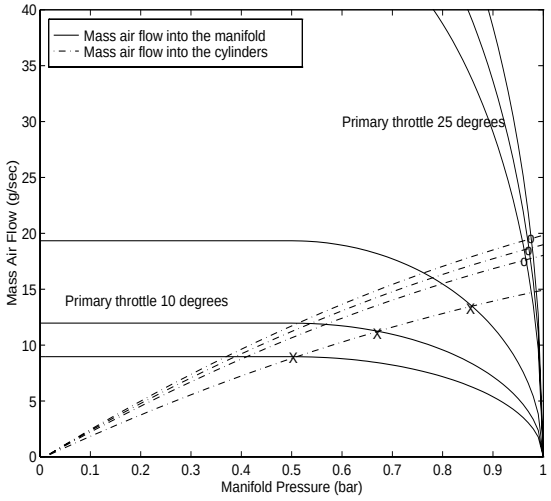

Figure 1: Operating points corresponding to primary throttle angle [9].

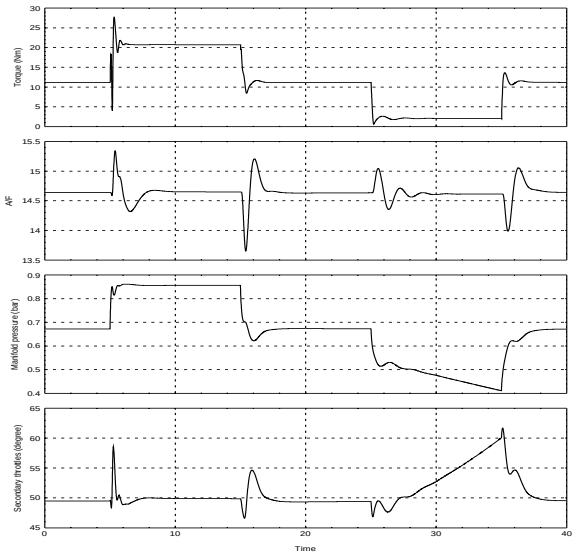

Figure 2: Simulation of linear control: step responses at low primary throttle angle (10^o), engine speed 300 rad/sec.

2 Discrete Engine Model

The basic model of the engine plus secondary throttles used here follows the model of [9]. The main difference is that [9] worked in continuous time, and here, the independent variable is taken to be the crank-angle, and this is discretized by $\frac{\pi}{2}$ rad. Indeed, the discrete event based nature of the engine combustion process introduces time-varying delays depending on the engine speed, which motivates discretizing the model syncronized with the engine events [2], [11]. The continuous 4-cylinder engine model, suggested by Crossley and Cook [3], is discretized by an Euler approximation with periodic crank-angle, which corresponds to the beginning of each event.

The dynamic model of the intake manifold is based on the "Filling and Emptying model" described in [7]. In this approach, the manifold is regarded as a plenum with a constant volume, where the rate of change of the manifold pressure is proportional to the difference between the mass air flow rate into the manifold ($\dot{m}_\theta$) and that pumped out of the manifold into the cylinders ($\dot{m}_{cyl}$). This relation can be expressed as a first order differential equation,

$$\frac{d}{dt}P_m = K_m(\dot{m}_\theta - \dot{m}_{cyl}) \tag{1}$$

where $K_m = \frac{R \cdot T}{V_m}$, R is the specific gas constant, T is the manifold temperature, and V_m is the manifold volume. The Euler approximation based on periodic crank-angle sampling gives

$$\begin{aligned} \frac{P_m(k+1)-P_m(k)}{\Delta\theta_s} \cdot \frac{\Delta\theta_s}{\Delta t} &= \frac{P_m(k+1)-P_m(k)}{\Delta\theta_s} \cdot N(k) \\ &= K_m(\dot{m}_\theta(k) - \dot{m}_{cyl}(k)) \end{aligned} \tag{2}$$

where $\Delta\theta_s$ is crank-angle sampling period, and N(k) is engine speed.

The mass air flow rate into the intake manifold ($\dot{m}_\theta(k)$) through the throttle body is a function of the primary throttle angle ($\theta(k)$), the upstream pressure (P_o) and the downstream pressure, which is manifold pressure ($P_m(k)$). Upstream pressure is assumed to

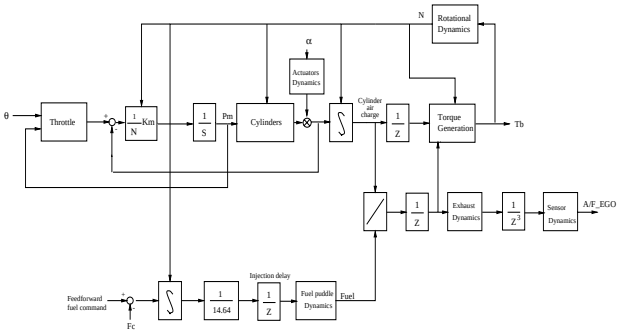

Figure 3: Nonlinear discrete engine model.

be atmospheric (i.e. P_o= 1 bar).

$$\begin{aligned}
\dot{m}_\theta(k) = \quad & f(\theta(k))g(P_m(k)) \\
f(\theta(k)) = \quad & 2.821 - 0.05231\theta(k) + 0.10299\theta(k)^2 \\
& -0.00063\theta(k)^3 \\
g(p_m(k)) & \\
= & \begin{cases} 1 & \text{if} \quad P_m(k) \le P_o/2 \\ \frac{2}{P_o}\sqrt{P_m(k)P_o - P_m(k)^2} & \text{if} \quad P_m(k) > P_o/2 \end{cases}
\end{aligned} \tag{3}$$

In a conventional engine, the mass air flow rate into the cylinders ($\dot{m}_f(k)$) is a function of manifold pressure ($P_m(k)$) and engine speed ($N(k)$), and for the engine under study is given by

$$\begin{aligned}
\dot{m}_f(k) = \quad & -0.366 + 0.08979N(k)P_m(k) \\
& -0.0337N(k)P_m(k)^2 + 0.0001N(k)^2P_m(k)
\end{aligned} \tag{4}$$

To include the secondary throttles, the conventional mass air flow rate into the cylinders is slightly modified as [9]

$$\dot{m}_{cyl}(k) = \theta_c(k) \cdot \dot{m}_f(k) \tag{5}$$

where $\theta_c(k)$ is limited from 0 (completely closed secondary throttles) to 1 (wide open secondary throttles). This provides control authority over the mass flow rate of air into the cylinders.

Remark : The cylinder air flow could also be regulated by variable intake valve timing, instead of secondary throttles. Essentially the same model would result.

Calculation delay in fuel injection and delays between the exhaust manifold and the EGO sensor are included in the discrete model, and the dynamics of EGO sensor and exhaust manifold are modeled by first order difference equations.

The steady state engine brake torque is affected by many parameters such as ignition delay, EGR and so on. To derive the general relations between these parameters and brake torque, experimental data are used along with curve fitting methods [2], [9].

$$\begin{aligned}
T_b = \quad & -181.3 + 379.36m_a + 21.91A/F - 0.85A/F^2 \\
& +0.26\sigma - 0.0028\sigma^2 + 0.027N - 0.000107N^2 \\
& +0.00048N\sigma + 2.55\sigma m_a - 0.05\sigma^2 m_a \\
& +2.36\sigma m_e \\
\text{where} & \\
m_a \quad & : \text{ mass air charge (g/intake event)} \\
A/F \quad & : \text{ air-fuel ratio} \\
N \quad & : \text{ engine speed (rad/sec)} \\
m_e \quad & : \text{ EGR (g/intake event)} \\
\sigma \quad & : \text{ degrees of spark advance before} \\
& \text{ top dead center}
\end{aligned} \tag{6}$$

For simplicity in the study, it is assumed that there is no EGR (i.e. m_e=0) and iginition (spark) delay (σ) is set to be 30^o.

3 Controller Architecture and Design

The control objective is to track torque demands imposed by the driver, while minimizing A/F excursions from stoichiometry. The controller inputs will be the secondary throttle "angle" and fuel. It is assumed that A/F is measured by a standard EGO sensor placed in the exhaust stream, just ahead of the catalyst. In addition, it is assumed that some means of measuring torque is available.

The difficulty of applying linear control is mainly due to the highly nonlinear nature of the manifold dynamics. In this section, a nonlinear feedforward feedback control design is outlined, based upon feedback linearization and gain scheduling. The basic idea is to write $\theta_c(k)$, the secondary throttles control signal, as a sum of two control signals, feedforward portion ($\theta_{cfw}(k)$) and feedback portion ($\theta_{cfb}(k)$).

The feedforward signal is chosen to approximately cancel the fast manifold dynamics that leads to A/F excursions, and substitute in a reference mass air flow model that has a speed of response that is more

within the means of the fuel controller. As an additional consideration, the reference model will be selected to lead to a higher nominal manifold pressure, thereby reducing pumping losses and increasing fuel economy. Model inaccuracies will inevitably lead to errors in the feedforward term. The primary goal of the feedback signal will be to attenuate these errors on the basis of measured torque and air-fuel ratio. A nice benefit of the feedforward control employed is that the feedback controller can be designed on the basis of a simplified model.

3.1 Model Based Feedforward Control

The key idea of the approach is to adjust $\theta_c(k)$ so that the mass air flow rate into the cylinders follows a reference model. The feedforward portion of the secondary throttles control signal is

$$\theta_{cfw}(k) = \frac{\dot{m}_{cyl}^{model}(k)}{\hat{\dot{m}}_f(k)}, \tag{7}$$

where $\dot{m}_{cyl}^{model}(k)$ is reference mass air flow rate into the cylinders, and $\hat{\dot{m}}_f(k)$ is an estimate of the mass air flow rate into the cylinders.

3.1.1 Estimate of Mass Air Flow Rate

The estimate of the mass air flow rate is based on the recent work in [6], and is expressed in terms of estimated manifold pressure ($\hat{P_m}(k)$) :

$$\hat{\dot{m}}_f(k) = \dot{m}_f(\hat{P_m}(k), N(k)) \tag{8}$$

The estimated manifold pressure ($\hat{P_m}(k)$) is derived from (2) and the direct measurement of $\dot{m}_\theta(k)$ from the hot-wire anemometer, whose dynamics are approximated as a first order lag with time constant τ. The Euler approximation of the pressure estimate is

$$\begin{aligned} &\frac{\hat{P_m}(k+1)-\hat{P_m}(k)}{\Delta\theta_s} \cdot N(k) \\ &= K_m(\frac{N(k)\tau}{\Delta\theta_s} MAF(k+1) - (\frac{N(k)\tau}{\Delta\theta_s} - 1)MAF(k) \\ &\quad -\theta_c(k) \cdot \dot{m}_f(\hat{P_m}(k), N(k)) \end{aligned} \tag{9}$$

where $MAF(k)$ is the measurement from the hot-wire anemometer. To remove the $MAF(k+1)$ term, define the new variable :

$$X(k) = \hat{P_m}(k) - K_m\tau MAF(k) \tag{10}$$

This yields an estimate of $P_m(k)$:

$$\begin{aligned} &\frac{X(k+1)-X(k)}{\Delta\theta_s} \cdot N(k) \\ &= K_m(MAF(k) - \theta_c(k) \cdot \dot{m}_f(\hat{P_m}(k), N(k)) \\ &\hat{P_m}(k) = X(k) + K_m\tau MAF(k) \end{aligned} \tag{11}$$

3.1.2 Reference Mass Air Flow Rate Model

The reference cylinder mass air flow rate model should be designed in consideration of fuel economy and torque characteristics. Here, the model is specified in terms of a derived steady state response, followed by a low pass filter. The steady state response is expressed in terms of the steady state manifold pressure $P_{ss}(\theta, N)$ of a conventional engine, primary throttle angle and engine speed :

$$\begin{aligned} &\dot{m}_{cyl,ss}^{model}(\theta, N) \\ &= \begin{cases} f(\theta)g(P_o/2+\delta) & \text{if} \quad P_{ss}(\theta,N)) \le P_o/2+\delta \\ f(\theta)g(P_{ss}(\theta,N)) & \text{if} \quad P_{ss}(\theta,N)) > P_o/2+\delta \end{cases} \end{aligned} \tag{12}$$

where δ is some small positive design constant. This yields the mass air flow characteristics of the secondary throttles engine being similar to those of a conventional engine at steady state. Furthermore, steady state manifold pressure is always kept higher than $P_o/2+\delta$, which decreases pumping losses without serious mass air flow reduction. δ is used as a tuning parameter for the offset of mass air flow reduction at low primary throttle angle. Finally, $\dot{m}_{cyl}^{model}(k)$ is generated by low-pass-filtering $\dot{m}_{cyl,ss}^{model}(\theta(k), N(k))$. The time constant of the low pass filter is determined, as a function of actuator dynamics, to minimize A/F excursions and maximize drivability. The reference torque is determined on the basis of the reference mass air flow model and engine speed, as shown in (6). This value will be used in a MIMO controller as a desired transient and steady state torque value.

3.2 MIMO Feedback Control

The potential benefits of the above feedforward control scheme will be lost if the mass air flow rate is not accurately estimated. Therefore, it is necessary

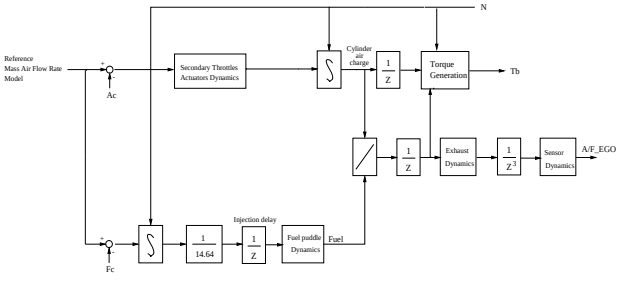

Figure 4: Open-loop engine model for feedback design.

to perform closed-loop compensation to keep the dynamics of the engine following the reference model as closely as possible.

The feedback signal is written as

$$\theta_{cfb}(k) = -\frac{A_c(k)}{\hat{\dot{m}}_f(k)} \tag{13}$$

The new control signal, A_c, is the feedback portion of the mass air flow rate into the cylinder. Figure 4 shows the open-loop configuration. Note that the highly nonlinear intake manifold dynamics is now ignored due to (7); that is, it is assumed that the estimated mass air flow rate is reasonably accurate. The inputs to the system are A_c and F_c, and the outputs are T_b and $(A/F)_{EGO}$.

3.2.1 Simplified Gain Scheduling

A robust MIMO control law for the system of Figure 4 is designed through the LQG/LTR methodology; the nominal model is linearized at a reference mass air flow rate equal to 20 g/sec, and engine speed equal to 300 rad/sec. To guarantee that steady state A/F and torque error are equal to zero, integrals of the torque and A/F errors are augumented to the linearized model in the LQG/LTR design procedure. The designed controller shows good performance over the range of the mass air flow rate from 5 g/sec to 80 g/sec, and engine speed from 200 rad/sec to 700 rad/sec. To improve its performance at low engine speeds, the simplified gain scheduling scheme of [5] is applied, regarding the reference mass air flow rate and engine speed as scheduling variables. The input gain matrix of this method is optimized along these variables, and scheduled to match the nominal loop gain over the range of the mass air flow rate from 10 g/sec to 30 g/sec, and the engine speed from 150 rad/sec to 500 rad/sec.

3.2.2 Reference Governor

The above design does not take into account that the control signal of the secondary throttles is limited from 0 (completely closed) to 1 (wide open). Hence, these actuators may saturate, deteriorating the system's response. During saturation, the integral state of the torque error winds up and adversely affects the fuel feedback control, due to the multivariable nature of the controller. It also causes undesirable overshoot in A/F response when the integral state finally unwinds.

One of the ways to surmount this difficulty is to introduce a supervisory loop which governs the reference mass air flow rate model so that the actuators are always driven to the non-saturation region [8]. To achieve this purpose, the following control law is suggested. First of all, note that the air flow freezes at the moment of saturation and it can be regarded as if that loop is open (broken) during saturation. In this condition, the excess air flow control signal during saturation (A_{sat}) can be expressed as :

$$A_{sat}(k) = (\theta_c(k) - sat(\theta_c(k)))\hat{\dot{m}}_f(k) \tag{14}$$

The idea is to use this portion of the control signal to cause the reference torque to track the actual engine torque by closing another loop so that torque error becomes zero during saturation, while the controller still updates the control signal.

Figure 5 demonstrates the new closed-loop configuration. When saturation occurs, $\theta_c(k)(= \theta_{cfw}(k) + \theta_{cfb}(k))$ can be expressed as follows :

$$\begin{aligned}
\theta_c(k) &= \frac{\dot{m}_{cyl}^{model}(k) - A_c(k)}{\hat{\dot{m}}_f(k)} \\
&= \frac{\dot{m}_{cyl,sat}^{model}(k) - A_{c,sat}(k)}{\hat{\dot{m}}_f(k)} + \frac{\dot{m}_{cyl,\Delta}^{model}(k) - A_{c,\Delta}(k)}{\hat{\dot{m}}_f(k)} \\
&= 1 + \frac{\dot{m}_{cyl,\Delta}^{model}(k) - A_{c,\Delta}(k)}{\hat{\dot{m}}_f(k)} = 1 + \frac{A_{sat}(k)}{\hat{\dot{m}}_f(k)}
\end{aligned} \tag{15}$$

During saturation, the system can be regarded as if it consists of the superposition of two subsystems shown

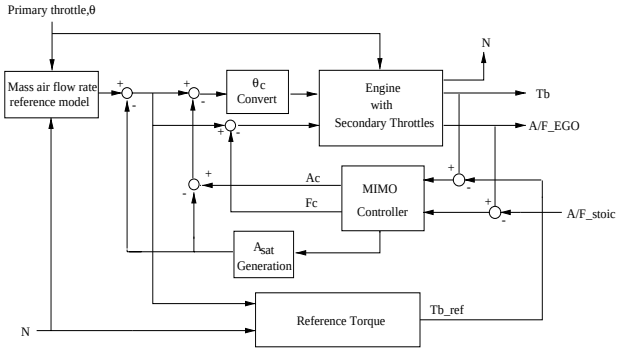

Figure 5: New closed-loop configuration.

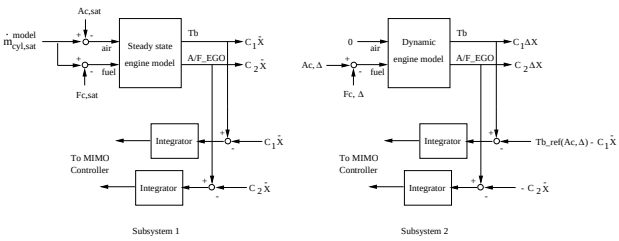

Figure 6: Schematic diagrams of two subsystems of proposed control during saturation.

in Figure 6. The states of subsystem 1 are the equilibrium points of the new closed-loop system when the reference mass air flow rate locates on the boundary of the non-saturation region, and those of subsystem 2 are dynamical deviations from the equilibrium states of subsystem 1. Through this new scheme, it can be shown that the observer errors from the LQG/LTR controller still converge to zero.

It is possible to choose the feedback gains in such a way that the unsaturated and saturated (subsystem 2) dynamics are simultaneously stabilized. From stability of the control loop around subsystem 2, it can be shown that $A_{c,\Delta}(k)$ converges to $-A_{c,sat}(k)$ to cancel the air flow error. Furthermore, in this case, the steady state value of θ_c is :

$$\theta_c = \frac{\dot{m}_{cyl,sat}^{model} + \dot{m}_{cyl,\Delta}^{model}}{\hat{\dot{m}_f}} = \frac{\dot{m}_{cyl}^{model}}{\hat{\dot{m}_f}} \qquad (16)$$

which means the secondary throttles cannot remain saturated in steady state when the steady state reference mass air flow rate is inside the non-saturation region.

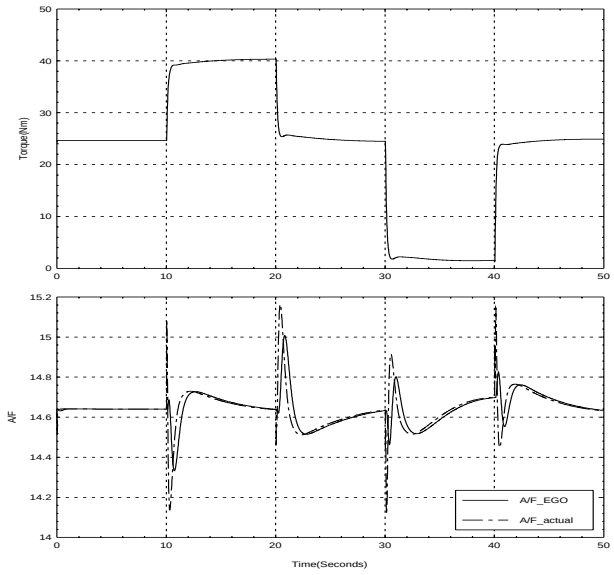

Figure 7: $\pm 4^o$ step responses at primary throttle angle 5^o, engine speed 100 rad/sec.

Remark : Simulations support the input to state stability of the overall control system, though this property has yet to be established analytically.

4 Simulation

To evaluate the performance of the proposed control scheme, the closed-loop system was simulated at engine speeds of 100 rad/sec and 400 rad/sec. The torque and engine speed are assumed to be measurable in real time, and step changes were given in the primary throttle angle. The simulation results demonstrate that the controller achieves good performance, though the system response is getting sluggish at low engine speed. The sluggishness is a consequence of doing the control design in the crank-angle domain. Indeed, the Nyquist frequency is proportional to the engine speed in the crank-angle based discrete system model. As a result, the controller's bandwidth width must be decreased as a function of engine speed, and this is done by the gain scheduler in the simulations.

To evaluate the reference governor, an improper reference mass air flow rate model was implemented

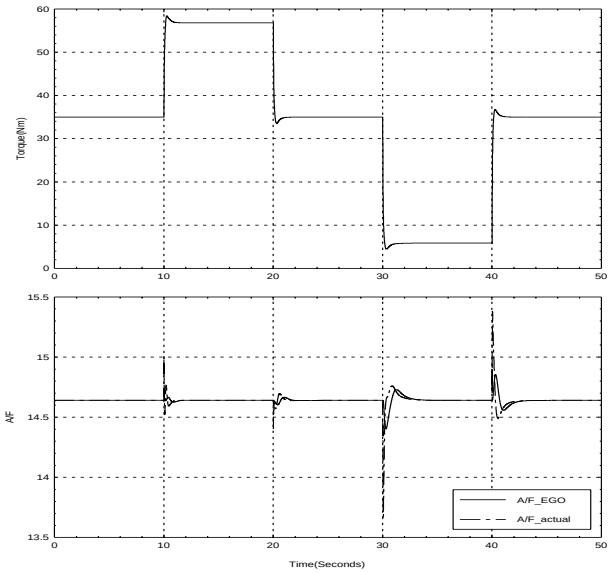

Figure 8: $\pm 4^o$ step responses at primary throttle angle 15^o, engine speed 400 rad/sec.

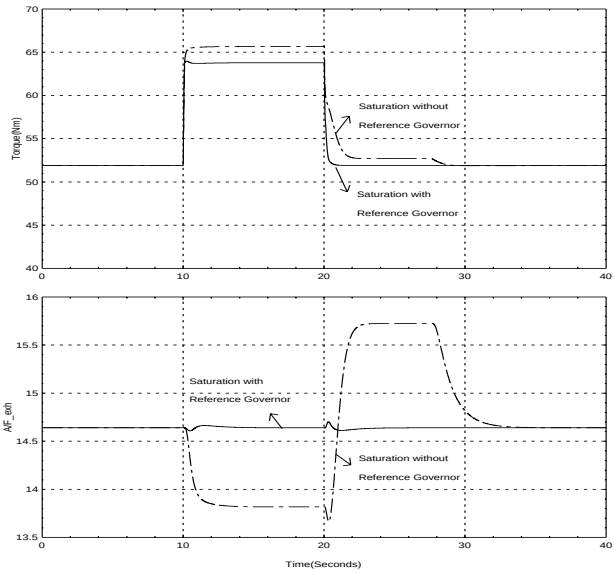

Figure 9: $+4^o$ step responses at primary throttle angle 15^o, engine speed 250 rad/sec.

on purpose, and simulated. The engine speed was set to 250 rad/sec, and 4^o step changes were given about a primary throttle angle of 15^o. The reference steady state torque is larger than maximum feasible torque at a primary throttle angle of 19^o. Figure 9 shows that closed-loop response is seriously deteriorated without the reference governor, due to actuator saturation (more extensive simulations even revealed instability of the system without the reference governor). On the other hand, it is seen that the effect of saturation is noticeably reduced by implementing the reference governor of Section 3.

5 Conclusions

In this paper, a nonlinear engine model equipped with secondary throttles at the intake runner was discretized with periodically with crank-angle, and a model based feedforward feedback control scheme was designed. It can be seen that a reasonably accurate estimate of mass air flow rate into the cylinders is critical to implement the suggested feedforward portion of the control scheme. The MIMO feedback control design was based on the linearized model, and to overcome actuator saturation, a reference governor was implemented. Finally, gain scheduling was performed to increase the domain of validity of the linear controller. The simulation results have shown favorable performance of the proposed controller over a wide range of operating points, thereby showing the potential of secondary throttles in enhancing engine performance without generating safety issues. In future work, we will investigate the input to state stability of the control scheme. Also, the control design will be improved to directly account for uncertainty in the mass air flow rate estimate.

Acknowledgements

The authors thank A. Stefanopolou and J. Cook of Ford Motor Company for helpful discussions. The work was supported by an NSF GOALI grant, ECS-9631237, with matching funds from Ford Motor Company.

References

[1] C. F. Chang, N. P. Fakete, and J. D. Powell. Engine air-fuel ratio control using an event-based observer. *SAE Paper*, (930766), 1993.

[2] J. A. Cook and B. K. Powell. Discrete simplified external linearization and analytical comparison of ic engine families. In *Proc. Amer. Contr. Conf., Minneapolis*, pages 325–333, June 1987.

[3] P. R. Crossley and J. A. Cook. A nonlinear model for drivetrain system development. In *IEE Conference 'Control 91', Edinburgh, U.K.*, volume 2, pages 921–925. IEE Conference Publication 332, March 1991.

[4] A. L. Emtage, P. A. Lawson, M. A. Passmore, G. G. Lucas, and P. L. Adcock. The development of an automotive drive-by-wire throttle system as a research tool. *SAE Paper*, (910081), 1991.

[5] S. Garg. A simplified scheme for scheduling multivariable controllers. *IEEE Control Systems Magazine*, pages 24–30, August 1997.

[6] J. W. Grizzle, J. A. Cook, and W. P. Milam. Improved transient air-fuel ratio control using air charge estimator. In *1994 American Control Conference*, volume 2, pages 1568–1572, June 1994.

[7] J. B. Heywood. *Internal Combustion Engine*. McGraw-Hill, 1988.

[8] P. Kapasouris, M. Athans, and G. Stein. Design of feedback control systems for stable plants with saturating actuators. In *Proc. IEEE Conf. Decision and Control, Austin, TX.*, pages 469–479, 1988.

[9] A. G. Stefanopoulou. *Modeling and Control of Advanced Technology Engines*. PhD thesis, University of Michigan, 1996.

[10] A. G. Stefanopoulou, J. W. Grizzle, and J. S. Freudenburg. Engine air-fuel ratio and torque control using secondary throttles. In *Proc. IEEE Conf. Decision and Control, Orlando*, pages 2748–2753, 1994.

[11] S. Yurkovich and M. Simpson. Comparative analysis for idle speed control: A crank-angle domain viewpoint. In *Proc. Amer. Contr. Conf., New Mexico*, pages 278–283, June 1997.